Nuclear Theory – Nuclear astrophysics

J.W. Holt

Introduction:

The structure, phases, and dynamics of nuclear matter are crucial to understand stellar explosions, the origin of the elements, patterns in observed gravitational waves, and the composition of the densest observable matter in the universe. The appropriate tool to study strongly interacting matter at the typical scales relevant in nuclear astrophysics (well below the scale of chiral symmetry breaking $\Lambda_\chi \approx 1$ GeV) is chiral effective field theory [1-3]. In recent years, chiral effective field theory has become a cornerstone of the modern approach to nuclear many-body dynamics that provides a systematic framework for describing realistic microphysics, such as multi-pion exchange processes and three-body forces, within a well-defined organizational hierarchy. The long and intermediate-range parts of the nuclear potential result from one- and two-pion exchange processes, while short-distance dynamics, not resolved at the wavelengths corresponding to typical nuclear Fermi momenta, are introduced as contact interactions between nucleons. Chiral effective field theory is unique in its multichannel methods for quantifying uncertainties and especially in its ability to estimate the importance of missing physics.

Optical potential comparison project

Large-scale astrophysical simulations are essential for identifying the site of the r-process, the primary candidates being the wind-driven ejecta from accretion disks surrounding binary neutron-star mergers or collapsars as well as the neutrino-driven winds of core-collapse supernovae. Neutron-capture rates on exotic neutron-rich isotopes are particularly important during the non-equilibrium freeze-out phase of r-process nucleosynthesis, but direct experimental studies at rare-isotope facilities remain unfeasible. The large uncertainties in these capture rates, due in part to difficulties in extrapolating phenomenological optical model potentials far from the valley of stability, limit the precision of predicted heavy-element abundances. Previously, we have constructed [4-6] from chiral effective field theory two- and three-body forces a microscopic global nucleon-nucleus optical potential with quantified uncertainties.

More recently, we have participated in a comparison project of optical potentials [7] to motivate future research directions in the field. In particular, we have clarified the important role of uncertainty quantification in both phenomenological and microscopic reaction theory calculations. In Fig. 1 we show the asymmetry in the total cross section for neutron scattering on ^{40}Ca and ^{48}Ca computed from several microscopic and phenomenological optical potentials. This quantity is a sensitive probe of the isospin dependence of the cross section away from stability, and we find that the microscopic calculation from chiral EFT (shown as the blue band) compares favorably to data as well as the phenomenological Koning-Delaroche optical potential with error analysis

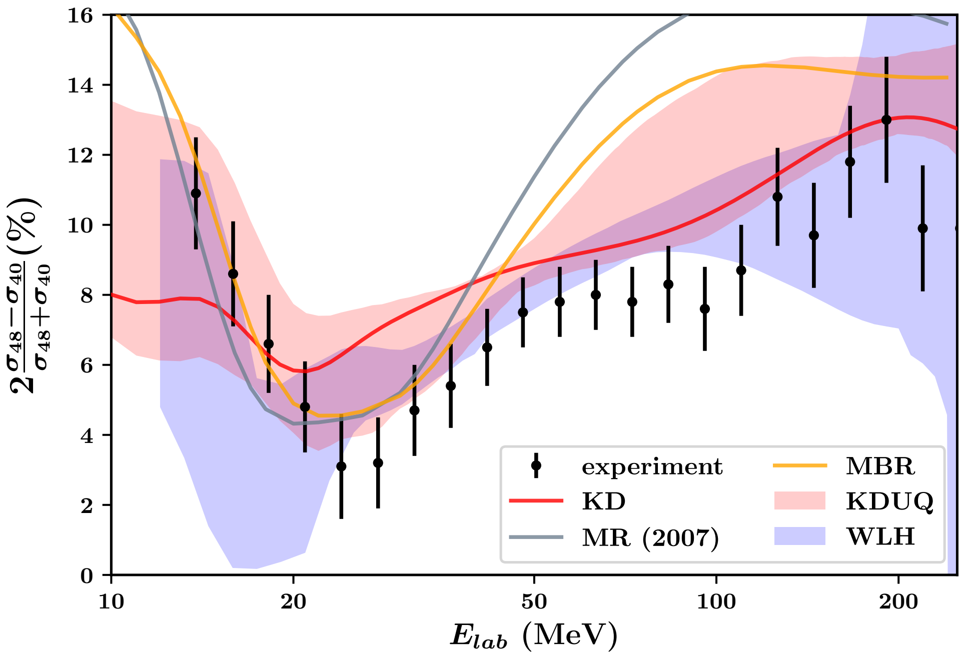

Fig. 1. Asymmetry of the total cross section between 40Ca and 48Ca. The shaded areas associated with the Koning-Delaroche (KDUQ) and Whitehead-Lim-Holt (WLH) global optical potentials correspond to 95% confidence intervals.

Neutron star properties from experimental and ab initio theory constraints of the ^{208}Pb Neutron Skin Thickness

Recent experimental and ab initio theory investigations of the ^{208}Pb neutron skin thickness are sufficiently precise to inform the neutron star equation of state. In particular, the strong correlation between the ^{208}Pb neutron skin thickness and the pressure of neutron matter at normal nuclear densities leads to modified predictions for the radii, tidal deformabilities, and moments of inertia of typical 1.4 solar-mass neutron stars. In recent work [8], we have studied the relative impact of these recent analyses of the ^{208}Pb neutron skin thickness on bulk properties of neutron stars within a Bayesian statistical analysis. Two models for the equation of state prior were employed in order to study the role of the highly uncertain high-density equation of state. From our combined Bayesian analysis of nuclear theory, nuclear experiment, and observational constraints on the dense matter equation of state, we found at the 90% credibility level $R_{1.4} = 12.36^{+0.38}_{-0.73}$ km for the radius of a 1.4 solar-mass neutron star, $R_{2.0} = 12.36^{+0.38}_{-0.73}$ km for the radius of a 2.0 solar-mass neutron star, $\Lambda_{1.4} = 440^{+103}_{-144}$ for the dimensionless tidal deformability of a 1.4 solar-mass neutron star, and $I_{1.338} = 1.425^{+0.074}_{-0.146} \times 10^{45}$g-cm^2 for the moment of inertia of PSR J0737-3039A whose mass is 1.338 solar masses. In Fig. 2 we show the probability distribution for a 1.4 $M_{\odot}$ neutron star starting, including only constraints from chiral effective field theory and nuclear masses, which is labeled by the blue “Prior” band. Individual posterior probability distributions that include constraints from gravitational wave data (GW170817), NICER radius measurements (NICER I and II), the experimental extraction of the

208Pb neutron skin thickness (PREX II), and the ab initio calculation of the ^{208}Pb neutron skin thickness (R_{np}^{th}) are shown as individual lines. Finally, the combined effect of all likelihood functions is shown as the red shaded band labeled “All”.

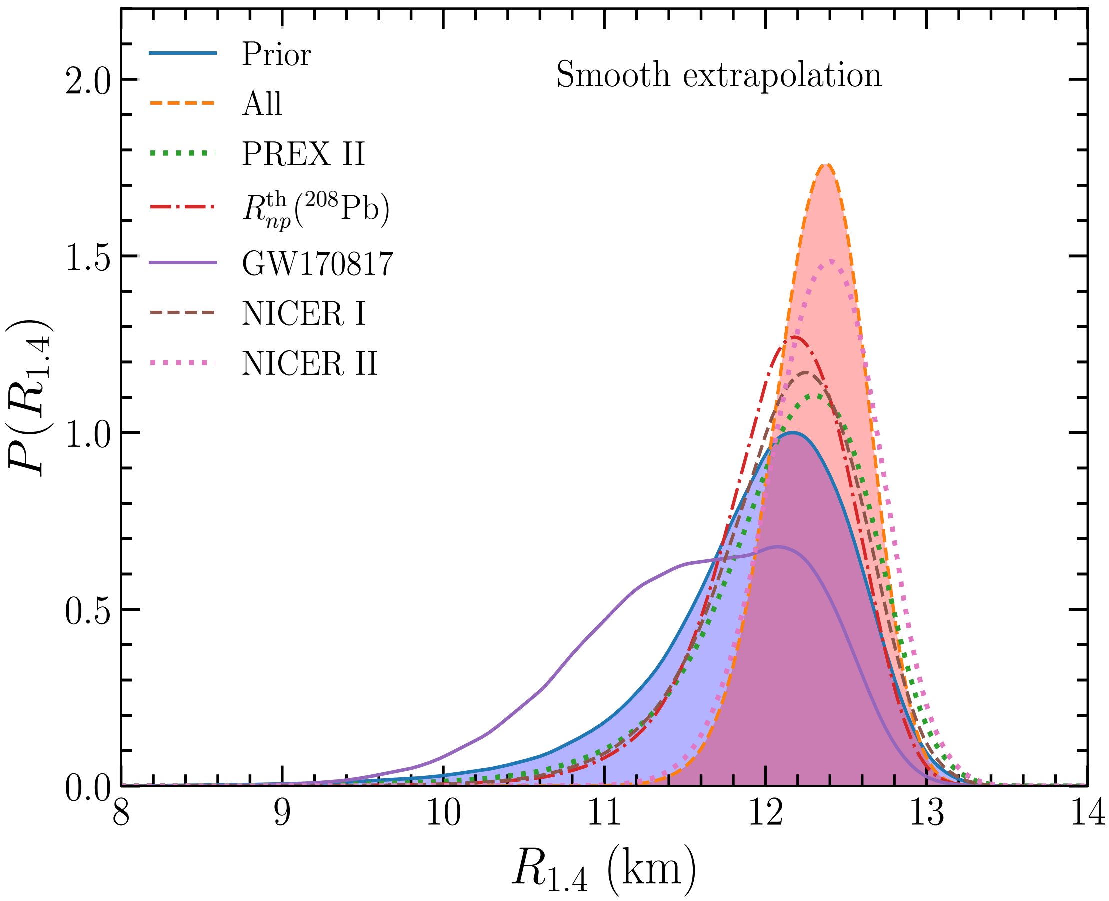

Fig. 2. Probability distribution for the radius of a $\mathbf{1.4}\ \boldsymbol{M_{\odot}}$ neutron star. The prior distribution is shown as the blue band, while the individual effect of various likelihood functions from gravitational wave (GW170817), electromagnetic (NICER I and II), and 208Pb neutron skin thickness predictions (PREX II and $\boldsymbol{R_{np}^{\mathrm{th}}}$) are shown as lines. The complete posterior including all likelihood functions is shown as the red band.

[1] S. Weinberg, Physica A **96**, 327 (1979).

[2] E. Epelbaum, H.-W. Hammer and U.-G. Meissner, Rev. Mod. Phys. **81**, 1773 (2009).

[3] R. Machleidt and D.R. Entem, Phys. Rept. **503**, 1 (2011).

[4] T.R. Whitehead, Y. Lim and J.W. Holt, Phys. Rev. C **100**, 014601 (2019).

[5] T.R. Whitehead, Y. Lim and J.W. Holt, Phys. Rev. C **101**, 064613 (2020).

[6] T.R. Whitehead, Y. Lim and J.W. Holt, Phys. Rev. Lett. **127**, 182502 (2021).

[7] C. Hebborn, F.M. Nunes, G. Potel, W.H. Dickhoff, J.W. Holt *et al.*, J. Phys. G. **50**, 060501 (2023).

[8] Y. Lim and J.W. Holt, Galaxies **10**, 99 (2022).